*AP*
ansta.eu

# PHOTODEGRADATION OF NAPHTHALENE BY NON-STOICHIOMETRIC TITANIUM OXIDES  MAGNELI PHASES

M. Marinkovski, P. Paunović,

J. Blaževska Gilev, J. G. Načevski

[1]Faculty of Technology and Metallurgy
University "Sts. Cyril and Methodius"
P.O. Box 580, MK-1001 Skopje, Republic of Macedonia
e-mail: pericap@tmf.ukim.edu.mk

**Abstract:**   This work is concerned with photochemical degradation of naphthalene using non-stoichiometric titanium oxides  Ebonex (Magneli phases). Ebonex was mechanically pretreated by milling in planetary mills for 20 h in order to reduce the particle size. For comparison, the photochemical degradation was performed by using of commercial photocatalyst $TiO_2$ HOMBIKAT UV-100. Structural characterization of the photocatalysts was performed by means of XRD analysis, Raman spectroscopy and SEM microscopy. It was found that HOMBIKAT UV shows anatase crystalline structure with particle size of 10 nm. Ebonex contains mostly the first three non-stoichiometric oxides of the homologues series: $Ti_4O_7$, $Ti_5O_9$ and $Ti_6O_{11}$ with particle size of about 200 nm. The both photocatalysts form spherical micron- or submicron-scaled aggregates. Photochemical activity within the UV region of the light was determined by means of FTIR spectroscopy. In both cases intensive activity was registered. However, Ebonex showed higher activity (the photocatalytic activity is more than 95%) related to the HOMBIKAT UV (the photocatalytic activity is near 60%). It is expected their photocatalytic activity to be more intensive in the visible region of the light.

**Key Words:**   Magneli phases, photocatalysis, $TiO_2$, naphthalene.

## 1. Introduction

Besides the industry, the source of organic pollutants emitted into environment can be many usual human activities such as driving a car, mowing grass, firewood for heating etc. Photocatalysis is a very promising method to solve many of the problems related to the increasing environmental pollution. Since the discover of the photoactivity of titania (early-1970s) an intensive development has made on the field of photochemistry. Recently, lot of attention is focused on nano-sized photocatalytic materials [1]. As a highly active, stable, non-toxic and cheap, $TiO_2$ is one of the most used photocatalysts in many fields of environmental remediation such as: decomposition of hazardous organic and malodorous compounds [2-4], purification and treatment of water [5] and air [5, 6], decolorization of dyeing waste-water [7, 8] etc. The photocatalytic activity of $TiO_2$ polymorphs is influenced by the type of crystalline structure, particle size and specific surface area, pore size and distribution etc. Among the polymorph phases of $TiO_2$ (brookite, anatase and rutile), anatase has shown the highest photocatalytic activity [9].

It is known that $TiO_2$ is photoactive in the UV region of light [10] which is less than 4% in solar light. It has been shown that addition (doping) of different anions or cations can effectively improve the photocatalytic activity of $TiO_2$ and promote it in the visible region of light [11-13]. This kind of activity is result of some lattice defects during the doping, mainly of oxygen vacancies. On the other hand, it is known that non-stoichiometric titanium oxides phases (Magneli phases) are formed by the introduction of oxygen vacancies into the $TiO_2$ structure in ordered arrangement [14]. So, this structure of Magneli phases offers their application in photocatalysis [15]. The main goal of the present work is application of Magneli phases as a photocatalyst for degradation of organic pollutants and to compare its activity with anatase crystalline form of $TiO_2$. As material  pollutant for photocatalytic degradation an aromatic hydrocarbon with two conjugated benzene rings  naphthalene was used. It was chosen as a hazardous pollutant which appears as by-product in the process of oil distillation, in emitted gases by vehicles etc.

## 2. Experimental procedures

As a photocatalysts for the oxidation of naphthalene non-stoichiometric titanium oxides (Magnelli phases) were used (trade name Ebonex, Altraverda, UK). For comparison, the photochemical degradation was performed by using of commercial photocatalyst $TiO_2$ HOMBIKAT UV-100. The used pollutant  naphthalene was supplied by Merck (p.a.). Because the used Magneli phases were graded in micron size (1÷5 $\mu m$), their application as photocatalyst would not have much effect. Therefore, firstly they were mechanically treated by Fritsch Planetary Mill (Pulverisisette 5) without binder. The dry ball milling was performed with acceleration of balls of 200 rpm, for different duration - 4, 8, 12, 16 and 20 h. The ball diameter was 1 cm, while the mass ratio of balls vs. treated material was 3:1. Photocatalytic materials previously were characterized by means of X-ray diffraction analysis (XRD), Raman spectroscopy and Scanning Electron Microscopy (SEM). XRD measurements were carried out by X-Ray diffractometer Philips APD 15, with $CuK_\alpha$ radiation. Raman spectroscopy measurements were performed using Nicolet Almega XR spectrometer (Thermo electron), with excitation line of 473 nm. SEM observation was carried out by JEOL JSM 6390 microscope equipped with an INCA Oxford Energy X-Ray Analyser. For oxidation of naphthalene pure oxygen was used. Equipment for the photocatalytic degradation of naphthalene was consisted of Pyrex glass vacuum line (pressure of 10-15 Pa). Within the line are connected solid naphthalene ($C_{10}H_8$) in a test tube with a valve, oxygen in a balloon and the photoreactor in which chemical vapor deposition taking place. The photocatalyst material is located onto glass carrier in the photoreactor. Mixture of oxygen and naphthalene was collected via vacuum line in Pyrex glass reactor before the UV irradiation. The excess gases were collected in renegade. The end of the vacuum line, vacuum pump was linked to achieve the required vacuum. For irradiation the mixture of naphthalene, oxygen and photocatalyst, mercury lamp was used (medium pressure and intensity of 100 W). To provide in-situ FTIR spectroscopy measurements, the ends of the reactor were supplied by KrS 5 (thallium bromide - thallium iodide) windows.

The change of the gas phase composition during the photocatalytic experiments was observed by means of FTIR spectroscopy (Nicolet Impact 400).

### 3. Results and Discussion

Determination of the particle size of the mechanically treated Magneli phases was done using TEM analysis. These results given elsewhere [16] are summarized in the diagram shown in Fig. 1. The particle size decreases from above 700 nm in the sample with untreated Magneli phases to 215 nm in the sample with Magneli phases treated for 20 h. The catalysts containing support material treated for 16 and 20 h show very close values of support's particle size, 230 and 215 nm respectively. So, the optimal duration of the mechanical treatment of Magneli phases would be in range of 16-20 h and further mechanical treatment is not necessary. This can be explained by the fact that during mechanical reduction of the particle size, the increase of the surface area is followed by considerably increase of the surface energy making the treated material thermodynamically unstable. The mechanism by which the material can be transferred to thermodynamically stable state (reduction of the overall energy) is agglomeration of the grains.
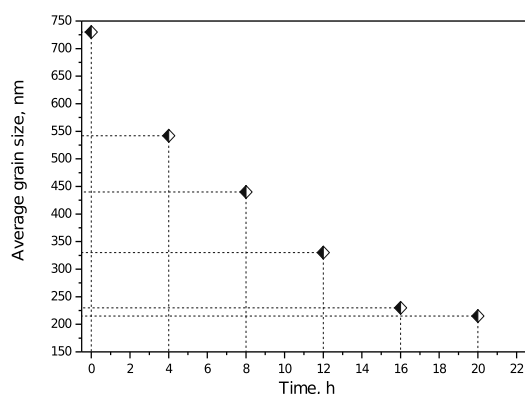


Figure 1: Plot of dependence between duration of mechanical treatment and average particle size of Magneli phases.

SEM images of both used photovatalysts are shown in Fig. 2. Magneli phases (Fig. 3a) forms aggregates in submicron dimensions and the presence of hole can be observed. This is suitable for inter-particle porosity of the material which is favorable for catalytic purposes. $TiO_2$ HOMBIKAT UV-100 (Fig. 3b) forms smaller aggregates ($50 \div 200$ nm) and its real surface area is obviously considerably higher (declared BET surface area is 250 $m^2g^{-1}$).
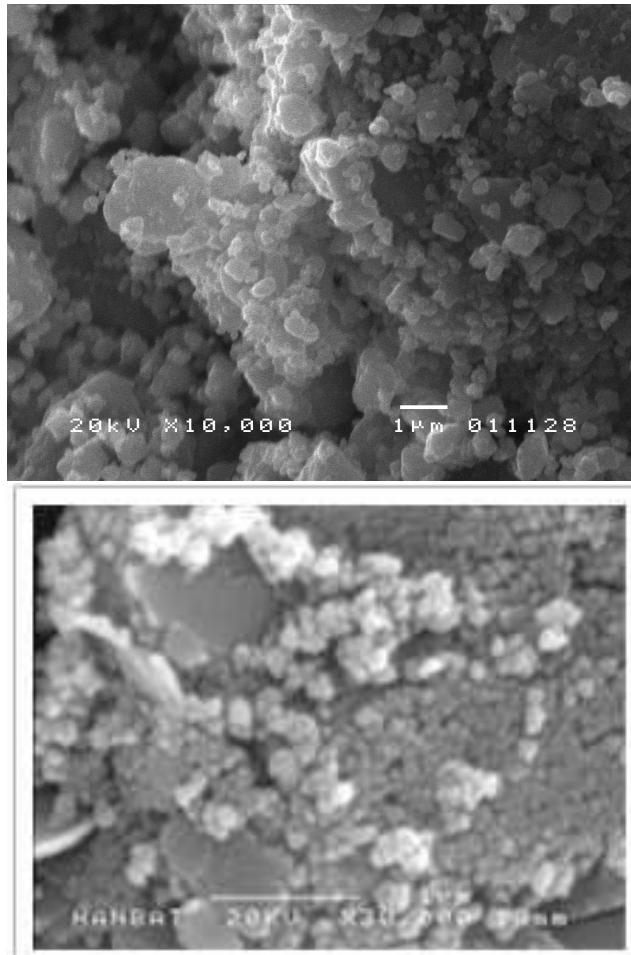
Figure 2: SEM images of a) Magneli phases and b) TiO$_2$ HOMBIKAT UV-100.
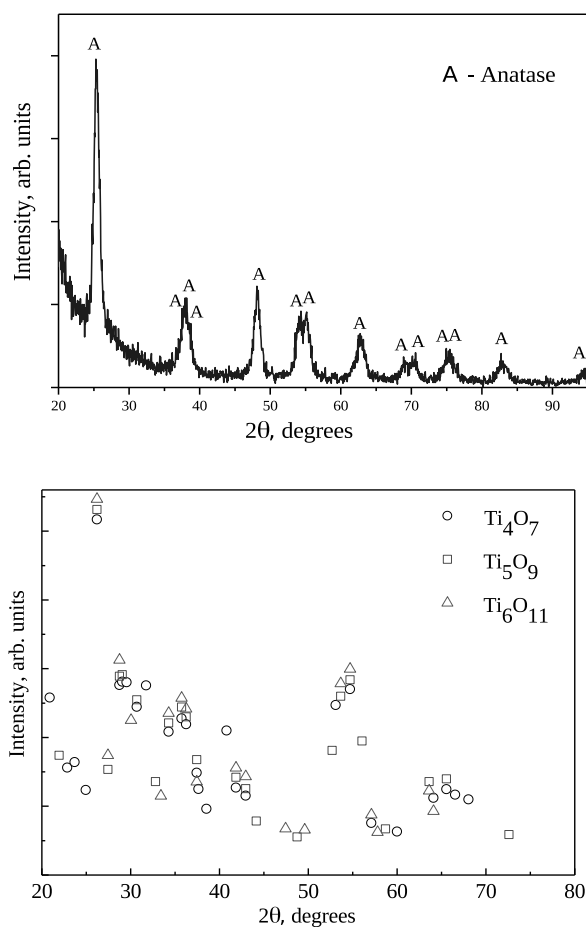
Figure 3: XRD spectra of a) Magneli phases and b) TiO$_2$ HOMBIKAT UV-100.

Phase composition of the photocatalysts was determined by means of X-ray diffraction analysis (XRD). XRD spectrum of HOMBIKAT UV-100 is shown in Fig. 3a.. As can be seen, all identified peaks corresponding to the anatase crystal structure of TiO$_2$. Fig. 3b shows the XRD spectrum of Magneli phases. It is known that the homologous series of Magneli phases (Ti$_n$O$_{2n-1}$ ($4 \leq n \leq 9$) is large [14] and in the studied material are present almost all oxides, more or less. According to the presented XRD spectrum, the first three oxides (Ti$_4$O$_7$, Ti$_5$O$_9$ and Ti$_6$O$_{11}$) of Magneli phases were detected. Their contribution is almost uniform. This does not mean that others homologous oxides are not present, but they are present in very small amounts.

The same phase composition for both photocatalysts was detected by Raman spec-
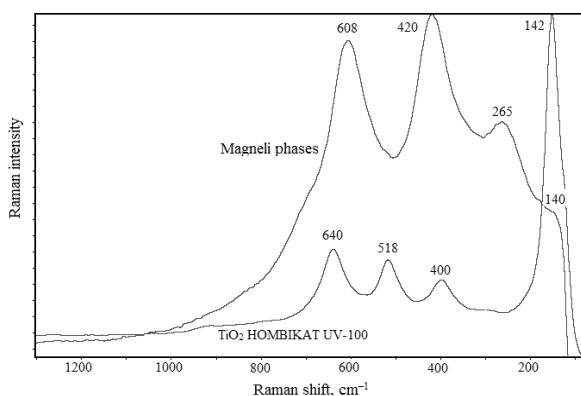
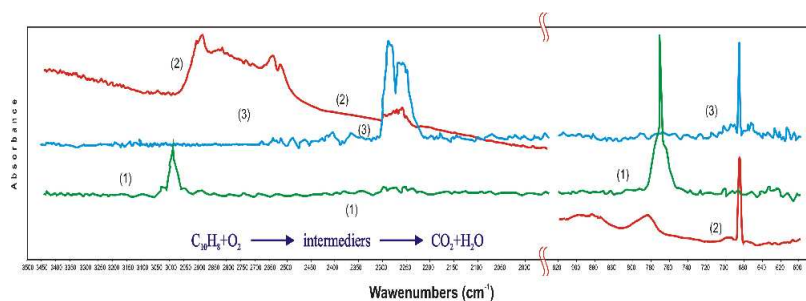Figure 4: Raman spectra of the studied photocatalysts.



Figure 5: FTIR spectra of naphthalene before irradiation (1) and after 180 min irradiation by $TiO_2$ HOMBIKAT UV-100 (2) and Magneli phases (3).

troscopy (Fig. 4). As can be seen, the photocatalyst TiO2 HOMBIKAT UV (curve 1) shows characteristic Raman bands (640, 518, 400 and 142 $cm^{-1}$) which correspond to the active modes of anatase crystalline structure [17, 18]. Within the Raman spectrum for Magneli phases (curve 2) characteristic bands were detected at 608, 420, 265 and 140 $cm^{-1}$. According to literature data [19, 20], these bands correspond to Magneli phases, i.e. to the first three of the homologous series: $Ti_4O_7$, $Ti_5O_9$ and $Ti_6O_{11}$. Raman spectra for both studied photocatalytic materials are in agreement with XRD analysis.

Photocatalytic degradation rate of naphthalene was observed by means of FTIR spectroscopy. Naphthalene oxidation is taking a place by the following reaction: $C_{10}H_8$ + $O_2$ + h$\nu$ + photocatalyst $\rightarrow$ intermediares $\rightarrow$ $CO_2$ + $H_{20}$ + photocatalyst Shown in Figure 5 are the FTIR spectra of naphthalene before irradiation (line 1) and after 180 min irradiation by $TiO_2$ HOMBIKAT UV-100 (line 2) and Magneli phases (line 3).

The line (1) shows that naphthalene has several characteristic peaks: peak with a medium intensity at 3060,3 $cm^{-1}$, peak with low intensity at 1263,4 $cm^{-1}$, peak with very high intensity at 781,8 $cm^{-1}$ and peak with high intensity at 473,3 $cm^{-1}$. After 3 h irradiation by UV-lamp in presence of commercial $TiO_2$ HOMBIKAT UV-100, FTIR spectra of degraded naphthalene is shown by line (2) in Figure 6. The peak at 3066 $cm^{-1}$ is almost disappeared, but as result of that it appear broad peak in the region from 3040÷2660 $cm^{-1}$ with a few pronounced maximums at 2970, 2900, 2733 and 2705 $cm^{-1}$. The first one (2970 $cm^{-1}$) corresponds to C-H stretching from aliphatic hydrocarbons [21]. The next peak positioned at 2900 $cm^{-1}$ appears as result of $CH_3$ stretching from aliphatic hydrocarbons. The peaks at 2733 $cm^{-1}$ and 2705 $cm^{-1}$ are consequence of aliphatic aldehyde $CH_2$-CHO [21]. The peak in the region of 2400 ÷ 2300 $cm^{-1}$ corresponds to a surface $CO_2$2 [22]. The peak 781,8 $cm^{-1}$ (characteristic one for naphthalene) is reduced for about 60%, and as a consequence of that a new peak at 668 cmv appears which corresponds to $CO_2$. FTIR spectra of degraded naphthalene after 3 h irradiation by UV-lamp in presence of Magneli phases, is shown by line (3) in Figure 5. It can be seen that peak at 3066 $cm^{-1}$ is totally disappeared which is result of degradation of aromatic rings. In the region of 2400 ÷ 2300 $cm^{-1}$ very pronounced peak exists as result of surface $CO_2$ [22]. Peak 781,8 $cm^{-1}$ (characteristic one for naphthalene) is disappeared (reduced more than 95%), and consequently new peak appears at 668 $cm^{-1}$ which corresponds to free $CO_2$ [22].

## 4. Conclusions

The research presented in this paper, was motivated by the idea to perform phocatalytic degradation of organic pollutant naphthalene by non-stoichiometric titanium oxides Magneli phases. This photodegradation was compared with corresponding one performed by commercial $TiO_2$ photocatalyst HOMBIKAT UV-100 with anatase crystalline structure. Structural characterization of the used photocatalysts was done by means of XRD analysis, Raman spectroscopy and SEM observation, while the processes of photocatalytic degradation was observed by FTIR spectroscopy. According to the exposed results, we could draw the following conclusions: $TiO_2$ HOMBIKAT UV is consisted of anatase crystals, which form spherical aggregates of 50÷200 nm. Magneli phases after 20 h milling reach submicron particles of about 200 nm. It was shown that further milling would not contribute to additional reduction of particles. Morphology of the Magneli phases was consisted of spherical aggregates of submicron and micron scale. After degradation of naphthalen for 3 h, in presence of HOMBIKAT UV, a lot of compounds in the gas mixture was detected such as unreacted naphthalen, substituted derivates of naphthalen and aliphatic hydrocarbons (ethanol, aldehides and ketones). After degradation of naphthalen for 3 h, in presence of Magnely phases, only $CO_2$ and water into the reactor was detected, indicating almost total degradation of aromatic hydrocarbon naphthalene. For total degradation of naphthalene in presence of Magneli phases the level of degradation was determined over than 95%, while in presence of HOMBIKAT UV corresponding degradation was less than 60%.

## References

[1] J. P. Wilcoxon, and B. L. Abrams, Nanosized Photocatalysts in Environmental Remediation, Nanotechnology, 2010, 51124.

[2] H. Hidaka, H. Nagaoka, K. Nohara, T. Shimura, S. Horikoshi, J. Zhao and N. Serpone, A mechanistic study of the photoelectrochemical oxidation of organic compounds on a $TiO_2$/TCO particulate film electrode assembly, J. Photochem. Photobiol. A: Chem., 98, 1996, 73-78.

[3] I. Sopyan, M. Watanabe, S. Murasawa, K. Hashimoto and A. Fujishima, An efficient $TiO_2$ thin-film photocatalyst: photocatalytic properties in gas-phase acetaldehyde degradation, J. Photochem. Photobiol. A: Chem., 98, 1996, 79-86.

[4] E. Pelizzetti and C. Minero, Mechanism of the photo-oxidative degradation of organic pollutants over $TiO_2$ particles, Electrochim. Acta, 93, 1993, 47-55.

[5] D.F. Ollis and H. Al-Ekabi (Eds.), Photocatalytic Purication and Treatment of Water and Air, Elsevier, Amsterdam, 1993.

[6] T. Mizuno, K. Adachi, K. Ohta and A. Saji, Effect of $CO_2$ pressure on photocatalytic reduction of $CO_2$ using $TiO_2$ in aqueous solutions, J. Photochem. Photobiol. A: Chem., 98, 1996, 87-90.

[7] J. Grzechulska and A. W. Morawski, Photocatalytic decomposition of azo-dye acid black 1 in water over modified titanium dioxide, Appl. Catal. B: Envir., 36, 2002, 45-51.

[8] A. J. Attia, S. H. Kadhim and F. H. Hussein, Photocatalytic Degradation of Textile Dyeing Wastewater Using Titanium Dioxide and Zinc Oxide, E-Journal of Chemistry, 5, 2008, 219-223.

[9] Z. Ambrus, K. Mogyorsi, . Szalai, T.Alapi, K. Demeter, A. Dombi and P. Sipos, Low temperature synthesis, characterization and substrate-dependent photocatalytic activity of nanocrystalline $TiO_2$ with tailor-made rutile to anatase ratio, Appl. Catal. A: General, 340, 2008, 153-161.

[10] K. Hashimoto, H. Irie and A. Fujishima, $TiO_2$ Photocatalysis: A Historical Overview and Future Prospects, Japan. J. of Appl. Phys., 44, 2005, 8269-8285.

[11] Y. Choi, T. Umebayashi and M. Yoshikawa, Fabrication and characterization of C-doped anatase $TiO_2$ photocatalysts, J. Mater. Sci., 39, 2004, 18371839.

[12] T. Ohno, M. Akiyoshi, T. Umebayashi, K. Asai, T. Mitsui and M. Matsumura, Preparation of S-doped $TiO_2$ photocatalysts and their photocatalytic activities under visible light, Appl. Catal. A: General, 265, 2004, 115-121.

[13] T. Ohno, T. Tsubota, M. Toyofuku and R. Inaba, Photocatalytic activity of a $TiO_2$ photocatalyst doped with $C^{4+}$ and $S^{4+}$ ions having a rutile phase under visible light, Catal. Lett., 98, 2004, 255-258.

[14] J. R. Smith, F. C. Walsh and R. L. Clarke, Electrodes based on Magnli phase titanium oxides: the properties and applications of Ebonex materials, J. Appl. Electrochem., 28, 1998, 10211033.

[15] M. Toyoda, T. Yano, B. Tryba, S. Mozia, T. Tsumura, M. Inagaki, Preparation of carbon-coated Magneli phases $Ti_nO_{2n-1}$ and their photocatalytic activity under visible light, Appl. Catal. B: Environment, 88, 2008, 160-164.

[16] P. Paunović, O. Popovski, E. Fidančevska, B. Ranguelov, D. Stoevska Gogovska, A. T. Dimitrov, S. Hadži Jordanov, Co-Magneli phases electrocatalysts for hydrogen/oxygen evolution, Int. J. Hydr. Ener., 35, 2010, 10073-10080.

[17] T. Oshaka, F. Izumi and Y. Fujiki, Raman spectrum of anatase, $TiO_2$, J. Raman Spectroscopy, 7, 1978, 321-324.

[18] H.C. Choi, Y.M. Jung and S. B. Kim, Size effects in the Raman spectra of $TiO_2$ nanoparticles, Vib. Spec., 37, 2005, 3338.

[19] A. Skopp, N. Kelling, M.Woydt and L.-M. Berger, Thermally sprayed titanium suboxide coatings for piston ring/cylinder liners under mixed lubrication and dry-running conditions, Wear, 262, 2007, 1061-1070.

[20] X. Li, A. L. Zhu, W. Qu, H. Wang, R. Hui, L. Zhang and J. Zhang, Magneli phase $Ti_4O_7$ electrode for oxygen reduction reaction and its implication for zinc-air rechargeable batteries, Electrochim. Acta, 55, 2010, 5891-5898.

[21] D. Byun, Y. Jin, B. Kim, J.K. Lee and D. Park, Photocatalytic $TiO_2$ deposition by chemical vapor deposition, J. Hazar. Mater., 73, 2000, 199206.

[22] I. Jogi, K. Kukli, J. Aarik, A. Aidla and Jun Lu, Precursor-dependent structural and electrical characteristics of atomic layer deposited films: Case study on titanium oxide, Mater. Sci. Semicon. Proc., 9, 2006, 10841089.